Highly Resolved Fluid Flows: "Liquid Plasmas" at the Kinetic Level

Gregor E. Morfill,* Milenko Rubin-Zuzic, Hermann Rothermel, Alexei V. Ivlev, Boris A. Klumov, Hubertus M. Thomas, and Uwe Konopka

Centre for Interdisciplinary Plasma Science, Max-Planck-Institute for Extraterrestrial Physics, 85741 Garching, Germany

Victor Steinberg

Department of Physics of Complex Systems, Weizmann Institute of Science, 76100 Rehovot, Israel

(Received 27 November 2003; published 28 April 2004)

Fluid flow around an obstacle was observed at the kinetic (individual particle) level using "complex (dusty) plasmas" in their liquid state. These "liquid plasmas" have bulk properties similar to water (e.g., viscosity), and a comparison in terms of similarity parameters suggests that they can provide a unique tool to model classical fluids. This allows us to study "nanofluidics" at the most elementary—the particle—level, including the transition from fluid behavior to purely kinetic transport. In this (first) experimental investigation we describe the kinetic flow topology, discuss our observations in terms of fluid theories, and follow this up with numerical simulations.

DOI: 10.1103/PhysRevLett.92.175004 PACS numbers: 52.27.Lw, 47.20.Ft, 47.27.Nz

"Complex plasmas" consist of electrons, ions, charged microparticles, and a neutral gas background. The microparticles can be individually visualized. They interact electrostatically, with the mean particle separation being typically ~100 times the particle size. Hence, these systems are "optically thin" up to ~10 cm in depth and can be probed three dimensionally.

It was discovered some time ago that complex plasmas can exist in "liquid" and "crystalline phases" [1–3], as well as in the (better known) "gaseous" state. One of the interesting aspects is that although they are intrinsically multiphase systems, the rate of momentum exchange through binary (electrostatic) collisions between the microparticles can exceed that of other interactions (e.g., Epstein neutral gas drag) significantly — thus providing an essentially one-phase system (e.g., fluids) for kinetic studies [4]. It is this unique property of liquid plasmas that will be employed here to study the fluid flow around an obstacle at the most elementary, the individual particle, level. Of particular interest are kinetic investigations of boundaries, instabilities and the transition to turbulence, which is regarded as the outstanding problem in hydrodynamics [5,6]. Individual particle observations can provide crucial new insights — e.g., whether the basic hydrodynamical instabilities (Kelvin-Helmholtz, Rayleigh-Taylor, Tollmien-Schlichting, etc.) will survive on interparticle distance scales, and whether the transition to turbulence can be seen at the particle (kinetic) level.

We present measurements of liquid complex plasmas flowing around an obstacle of size ~100 mean particle separations (equivalent to ~100 "effective" particle diameters, or "molecular" distances). We observe stable laminar shear flow around the obstacle, the development of a "wake" exhibiting stable vortex flows, and an unstable mixing layer between the flow and the wake. Using simple dimensionless scaling relations we compare the liquid plasma measurements with classical fluid flows. This suggests that liquid plasmas can provide a unique quantitative approach towards understanding nanofluidics and any nonlinear processes occurring at this level.

The observations.—The experiments were carried out in a radio-frequency (rf) plasma chamber. Thermophoresis [7] was used to compensate for gravity. The microparticles (diameter $2a = 3.7 \pm 0.15$ μm) develop a steady axially symmetric flow pattern with an upward flow at the perimeter and a homogeneous uniform downward flow of diameter ~2 cm (velocity $u \simeq 0.8$ cm/s and density $n_d \simeq 1.3 \times 10^6$ cm^{-3}) along the chamber axis (Fig. 1). Individual particles are visualized through the reflected light from a narrow laser sheet, which illuminates a vertical plane of ~100 μm thickness passing through the chamber axis. The mean separation between the particles is $\Delta \simeq 90$ μm, which implies that typically only one particle plane is illuminated. The measured large ratio $\Delta/a \simeq 50$ allows us to look right into the system, it is transparent. The temporal development of the flow is recorded with a charge-coupled device camera at a rate of 15 Hz.

The "obstacle" is a lentil shaped "void"— a region in which plasma processes prevent particle penetration [8]. It is located in the center of the chamber and has been observed on numerous occasions, especially under microgravity conditions [9]. The size of the void can be adjusted using gas pressure and rf power. In the experiment shown here, the horizontal diameter was $L_x \simeq 0.9$ cm (corresponding to $\simeq 100\Delta$) and the vertical thickness was $L_z \simeq 0.57$ cm (corresponding to $\simeq 60\Delta$).

The main features are the following: Surrounding the void upstream, a laminar boundary layer is formed, which has a thickness of ~5Δ. In this layer the liquid plasma is compressed by a factor 3–5 compared to the overall flow regime, which had a uniform density (±30% variation) resembling incompressible fluid flow.

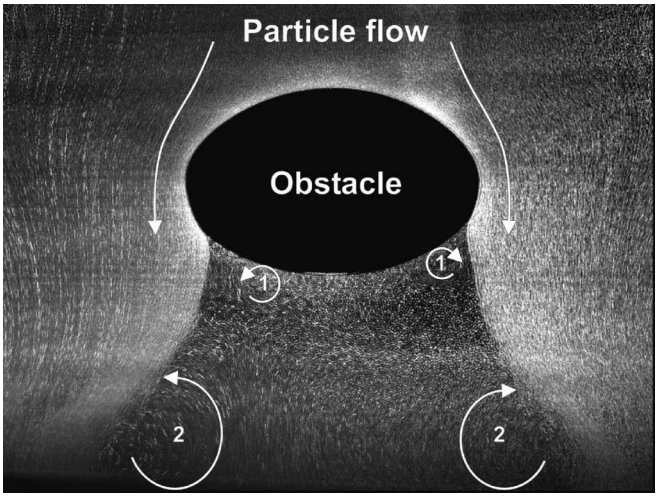

FIG. 1. Topology of the particle flow around the "void." The flow leads to a compressed laminar layer of thickness $\sim 5\Delta$. This layer becomes detached at the outer perimeter of the wake. The steady vortex flow patterns in the wake are illustrated. In terms of the (transverse) void dimension $L_x \simeq 100\Delta$, the vortices have the following cross sections: (1) area $\simeq 0.2L_x \times 0.1L_x \simeq 200\Delta^2$, (2) area $\simeq 0.3L_x \times 0.2L_x \simeq 600\Delta^2$. The boundary between laminar flow and wake becomes unstable, a mixing layer is formed which grows in width with distance downstream. The system is approximately symmetric around the vertical axis, the vortices are tori and the wake has the shape of a flaring funnel (size of image 2.05 cm × 1.50 cm, exposure time 1 s).

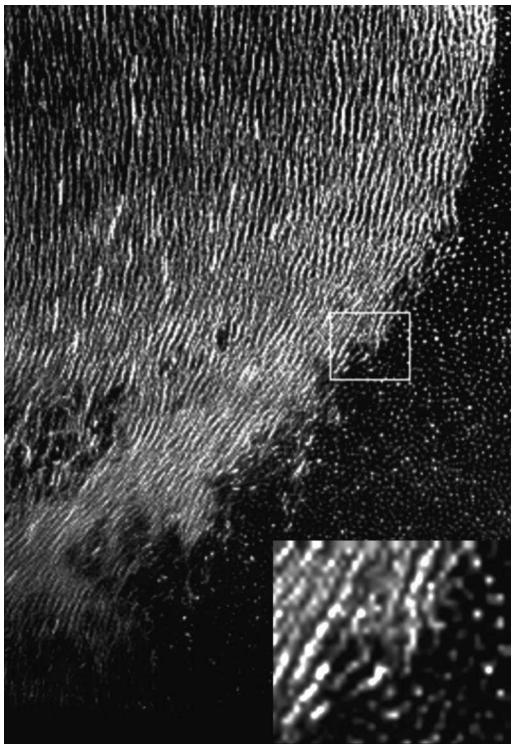

FIG. 2. An example of the mixing layer—an enlargement of the left side of the flow regime shown in Fig. 1 (size of image 0.51 cm × 0.75 cm size, exposure time 0.05 s). The points (lines) represent traces of slow (fast) moving microparticles. The particles are "overexposed," in reality the interparticle distance is ~25 times the particle diameter. The "liquid plasma" consists of argon ions, electrons, and the (charged) microparticles which are visible in the images. Neutral gas (argon) at 0.64 mbar provides some damping. The microparticles are the dynamically dominant component (mass density 5×10^{-5} g/cm^3), followed by the neutrals ($\sim 10^{-6}$ g/cm^3), the ions ($\sim 6 \times 10^{-14}$ g/cm^3), and the electrons ($\sim 10^{-18}$ g/cm^3). Interactions between the microparticles are electrostatic. The inset shows a magnified field, as indicated in the overview image.

The boundary layer covers about 70% of the void surface. The detachment line is remarkably stable, the position is fixed to within 2Δ, the angle of detachment is $45° \pm 15\%$. Behind the obstacle a wake is formed, which is separated from the laminar flow region by a mixing layer. Some momentum has to be transferred into the wake region, since adjacent to its boundary a vortex flow is established, with a rotation direction suggesting that the energy source is in the flow. The topology of the vortex is that of a torus. Further downstream there is a second vortex (torus) in the wake, which rotates in the same way, also suggesting the flow as the energy source. We will discuss this later.

The wake and the laminar flow regimes are separated by a mixing layer or transfer layer. In this region, momentum is transferred between the two fluid regimes leading, e.g., to the vortex flows mentioned above. It is clear from our observations—see the example shown in Fig. 2—that the boundary becomes unstable on kinetic (particle) scales [10]. Optically, the kinetic (particle) system looks no different at first sight than typical macroscopic wake flows rendered visible using tracers. We must remember, however, that here we are not seeing tracer fluids—we are observing individual strongly interacting particles—a kinetic fluid. The inset in Fig. 2 shows a magnified portion of the flow boundary: Although the individual microparticles are overexposed, exaggerating their size, we see that they are well separated. Fast flowing particles appear as lines for the exposure time used.

Characterization of the liquid plasma.—Let us compare liquid plasmas with classical fluids:

(i) The *shear viscosity* of strongly coupled Yukawa fluids has been determined from numerical simulations [11]. The kinematic viscosity is $\nu_d \simeq 10^{-2}$–10^{-1} cm^2/s (depending on the coupling strength and density)—a value similar to that of water ($\nu_w \sim 10^{-2}$ cm^2/s). The flow speed in our experiment was $u \simeq 0.8$ cm/s. This yields a Reynolds number for our system of $R = uL_x/\nu_d = 5$–50.

(ii) To determine the *Mach number*, we require the sound speed. In complex plasmas the relevant "sound wave" is the compressional "dust acoustic wave" [12]. The microparticles are charged, and compressional fluctuations are transmitted via electrostatic forces, as in usual plasmas. We estimate the dust acoustic speed to be $C_d \simeq 1.4$ cm/s, which yields a dust acoustic Mach number $M_d = u/C_d \simeq 0.5$.

(iii) To determine the *type of flow* observed, we calculated the ratio $\eta =$ (momentum exchange rate by binary collisions)/(Epstein drag with the neutral gas). A large value for η implies a one-phase flow, dominated by the microspheres. From collision theory [4] we have

$$\eta = \frac{1}{2}\frac{\rho_d \delta v_d}{\rho_n v_{T_n}}\left(\frac{\lambda}{a}\right)^2 \ln^2(2\beta), \tag{1}$$

where ρ defines the mass densities, δv_d the relative (mean) velocity between the particles, v_{T_n} the thermal velocity of the gas, and λ the plasma screening length. The so-called "scattering parameter,"

$$\beta \equiv \Gamma\kappa, \tag{2}$$

which is a function of the particle charge number Z_d and temperature T_d, is conveniently expressed in terms of the coupling parameter $\Gamma = e^2 Z_d^2/\lambda T_d$ and lattice parameter $\kappa = \Delta/\lambda$. For the fluid state we have from theoretical considerations [13] $\Gamma e^{-\kappa}(1 + \kappa + \frac{1}{2}\kappa^2) < 106$, so that from Eqs. (1) and (2) we can derive upper limits for η. Using the measured values we obtain for $\kappa = 1$:

laminar flow regime ($\delta v_d \sim 0.1u$),	$\eta \leq 7.0$,
mixing layer ($\delta v_d \sim 0.5u$),	$\eta \leq 35.0$,
wake regime ($\delta v_d \sim v_{T_d}$),	$\eta \leq 5.0$,

where v_{T_d} is the particle thermal velocity at room temperature. For $\kappa = 2$ the limits are a factor 2.88 lower. We know from theoretical considerations that η has to be very close to these limits [13].

(iv) *Scaling our system* to a classical one-phase fluid, water, we use $\Delta_w \simeq 3 \times 10^{-8}$ cm and, hence, $\nu_w \sim 10^{-2}$ cm^2/s $\sim 10^{13}\Delta_w{}^2$/s. To get a Reynolds number of, say, 20, which is in the middle range of that estimated in our experiment, for an obstacle of width 100 Δ_w (i.e., $\simeq$ 30 nm), the water flow speed has to be $u_w \simeq 2 \times 10^{12}\Delta_w/\text{s} \simeq 550$ m/s. This gives a Mach number $M_w = u_w/C_w \simeq 0.4$, which is nearly the same as the dust acoustic Mach number derived for our complex plasma experiment.

Hence we may conclude that based on similarity parameters (R, M), the complex plasma fluid is remarkably like water—observed at the molecular level. This suggests that we have a powerful new tool for investigating fluid flows on (effectively) nanoscales, including the all-important transition from collective flow behavior to individual kinetic behavior, as well as nonlinear processes on small scales, that have not been accessible for studies so far. This promises to be an exciting future research field.

Driving mechanism for the vortex flow.—In the wake we obtained $\eta < 5$ for $\kappa = 1$ (or ≤ 1.7 for $\kappa = 2$), i.e., the wake is closest to being a multifluid regime. Accordingly, taking the momentum flux from the flow regime into the mixing (or transfer) layer to be the driving force, we solve the coupled momentum equations for ions, neutrals, and particles under the reasonable assumptions of constant pressures and charge neutrality, taking into account Epstein drag (with the coupling rate τ_f^{-1}) and viscous equilibration of the gas at the characteristic length scale $L = \frac{1}{2}\sqrt{L_x L_z}$. With largely self-explanatory notation we then have to solve

$$m_i \frac{dv_i}{dt} = -m_i n_n \sigma_{in} v_{T_n}(v_i - v_n) + eE, \tag{3}$$

$$m_n \frac{dv_n}{dt} = -m_n n_i \sigma_{in} v_{T_n}(v_n - v_i) - m_d \frac{n_d}{n_n}\tau_f^{-1}(v_n - v_d) - m_n \nu_n L^{-2} v_n, \tag{4}$$

$$m_d \frac{dv_d}{dt} = -m_d \tau_f^{-1}(v_d - v_n) - Z_d eE + F_{\text{mix}}, \tag{5}$$

$$j_d + j_e - j_i = (n_d Z_d v_d + n_e v_e - n_i v_i)e = \sigma E. \tag{6}$$

The driving force, F_{mix}, defined as (momentum flux into the mixing layer)/(number of particles in the vortex), acts only on the microspheres

$$F_{\text{mix}} = \xi \frac{m_d l u^2}{A}\frac{n_{d(f)}}{n_{d(w)}} \tag{7}$$

with l the thickness of the mixing layer, $\xi \simeq 0.5$ the mixing fraction, $A = L_x L_z$ the cross section of the vortex torus, and $n_{d(f)}/n_{d(w)}$ the ratio of the particle densities in the flow and wake regimes, respectively. The viscous dissipation (randomization) of the neutrals occurs at the rate ν_n/L^2 over a characteristic scale, $L \equiv \sqrt{A}$. The electric field, E, in the system is defined through the current Eq. (6)—the conductivity is dominated by electrons if $\sigma_e/\sigma_i < 1$, and by ions if $\sigma_e/\sigma_i > 1$. For argon gas with $T_i = 300$ K, $T_e = 3 \times 10^4$ K this gives $n_e/n_i > 4 \times 10^{-2}$ (or $n_e/n_i < 4 \times 10^{-2}$, respectively).

Neglecting small terms and assuming steady state, the set of Eqs. (3)–(7) reduces to

$$v_p = \xi\left(1 + \frac{\rho_d A}{\rho_n \nu_n \tau_f}\right)\frac{\tau_f l u^2}{A}. \tag{8}$$

This yields a theoretical estimate of the thickness of the mixing layer, l, in terms of known and measured quantities. We obtain $l_1 \sim \Delta$ for vortex system (1), and $l_2 \sim 10\Delta$ for vortex (2). In both cases the calculated mixing layer thickness is in agreement with observations. Considering the uncertainties we conclude that the measurements are compatible with the flow providing the energy source which drives the vortices in the wake.

Instability of the mixing layer.—The surface between the flow region and the wake is observed to be quite unstable at the kinetic level, with instabilities becoming rapidly nonlinear. The ensuing mixing layer grows monotonically with distance from the border where the laminar flow becomes detached from the obstacle. The growth length scale is of the order of a few Δ, i.e., much smaller than the hydrodynamic scales $\rho_d(d\rho_d/dz)^{-1}$ or $u(du/dz)^{-1}$, which would be expected macroscopically in fluids and refer to the Rayleigh-Taylor or Kelvin-Helmholtz instability, respectively. This rapid onset of

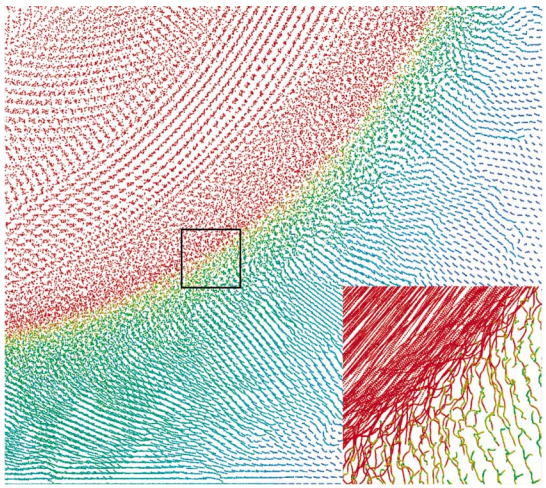

FIG. 3 (color). A numerical simulation of the mixing layer. Parameters used were similar to those of the experiment. Traces show particle displacements during $\simeq 0.06$ s which corresponds to the exposure time in the experiment. Particle velocities are color coded, increasing from blue to red.

surface instabilities followed by mixing and momentum exchange at scales $O(\Delta)$, i.e., the smallest interaction length scale (= effective particle size) available, is not consistent, therefore, with conventional macroscopic fluid instability theories. While this could not rightfully be expected at the kinetic level, it clearly points to new physics and, possibly, a hierarchy of processes that is necessary to describe interacting fluid flows: first, binary collision processes provide particle and momentum exchange on kinetic scales (a few Δ), then collective effects (due to the correlations defining fluid flows) take over and "propel" this "seed" instability to macroscopic scales (mean Δ).

The microscopic driving mechanism for the observed instabilities in the mixing layer is identified as a new type of nonlinear collisional instability, inertially driven by binary (electrostatic) collisions. The wake boundary curves outwards, and over the whole downstream distance, particles are deflected by 40°–50° on average. It appears that, statistically, some particles manage this via multiple small angle collisions and some particles end up undergoing large angle ($>30°$) collisions in the surface layer. These then have a high probability of transferring to (and being absorbed by) the wake regime and vice versa. As the surface becomes rougher (and larger) these binary collisions become more important, driving the instability into a nonlinear state. We have conducted numerical simulation studies to test this interpretation, using a molecular dynamics code with a repulsive Yukawa potential between the particles. The result for similar geometry and flow conditions as in the experiment is shown in Fig. 3. The topology of the mixing layer corresponds closely to the measurements, which supports our kinetic interpretation.

Summary.—We have observed fluid flow around an obstacle at the kinetic (particle) level for the first time. The boundary layer around the obstacle appears to be frictionless—a "slip boundary"—presumably due to the fact that its microroughness is much less than the effective particle size, $\simeq \Delta/2$. The most interesting feature is the mixing layer between the flow and wake, which exhibits instability growth on scales much smaller than the hydrodynamic scale, if we identify this as the density or shear velocity gradient along the flow lines. The solution to this puzzle is probably due to the curved flow driving a collisional instability, which has been observed for the first time at the kinetic level. Numerical simulations have confirmed that interface instabilities on particle separation scales $O(\Delta)$ may indeed occur under such circumstances. Finally, we showed that the momentum transfer in the mixing layer, as observed, is compatible with driving the vortex flows seen in the wake behind the obstacle.

This work was supported by DLR/BMBF under Grant No. 50WM9852 (PKE-Nefedov) and 50WP0203 (PK-3 Plus). The authors wish to acknowledge the excellent support from the PKE-Nefedov team and the agencies involved in making PKE-Nefedov a success: DLR, Rosaviakosmos, the Russian Ministry of Industry, Science and Technologies, the Russian Foundation for Basic Research, TSUP, RKK-Energia, Kayser-Threde, TSPK, IPSTC, and the cosmonauts.

*To whom correspondence should be addressed.
Email address: gem@mpe.mpg.de

[1] H. Thomas *et al.*, Phys. Rev. Lett. **73**, 652 (1994).
[2] J. H. Chu and Lin I, Phys. Rev. Lett. **72**, 4009 (1994).
[3] H. M. Thomas and G. Morfill, Nature (London) **379**, 806 (1996).
[4] S. A. Khrapak, A. V. Ivlev, and G. E. Morfill, "Momentum Transfer in Complex Plasmas" (to be published).
[5] P. Drazin and w. Reid, *Hydrodynamic Stability* (Cambridge University Press, Cambridge, 1981).
[6] M. Lesieur, *Turbulence in Fluids* (Kluwer Academic Publ., Dordrecht, 1991).
[7] H. Rothermel *et al.*, Phys. Rev. Lett. **89**, 175001 (2002).
[8] G. E. Morfill *et al.*, in *Dusty Plasmas in the New Millennium—2002*, Proceedings of the 3rd International Conference on the Physics of Dusty Plasmas, AIP Conf. Proc. No. 649 (AIP, New York, 2002), pp. 91–109.
[9] G. E. Morfill *et al.*, Phys. Rev. Lett. **83**, 1598 (1999).
[10] More details can be found in the movie, which, can be accessed under http://www.mpe.mpg.de/complex-plasmas/movies/flow.html
[11] T. Saigo and S. Hamaguchi, Phys. Plasmas **9**, 1210 (2002).
[12] N. N. Rao, P. K. Shukla, and M. Y. Yu, Planet. Space Sci. **38**, 543 (1990).
[13] O. S. Vaulina and S. A. Khrapak, JETP **90**, 287 (2000).